Accepted Manuscript

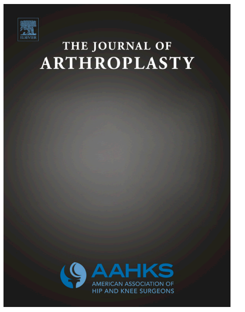

Application of far cortical locking technology in periprosthetic femoral fracture fixation - a biomechanical study

Mehran Moazen, PhD, Andreas Leonidou, MSc, Joseph Pagkalos, MSc, Arsalan Marghoub, MSc, Michael J. Fagan, PhD, Eleftherios Tsiridis, MD, MSc, PhD, FRCS

PII: S0883-5403(16)00133-9

DOI: 10.1016/j.arth.2016.02.013

Reference: YARTH 54963

To appear in: *The Journal of Arthroplasty*

Received Date: 7 May 2015

Revised Date: 6 January 2016

Accepted Date: 8 February 2016

Please cite this article as: Moazen M, Leonidou A, Pagkalos J, Marghoub A, Fagan MJ, Tsiridis E, Application of far cortical locking technology in periprosthetic femoral fracture fixation - a biomechanical study, *The Journal of Arthroplasty* (2016), doi: 10.1016/j.arth.2016.02.013.

Application of far cortical locking technology in periprosthetic femoral fracture fixation - a biomechanical study

Mehran Moazen, PhD[1]
Andreas Leonidou, MSc[2]
Joseph Pagkalos, MSc[2]
Arsalan Marghoub, MSc[1]
Michael J Fagan, PhD[3]
Eleftherios Tsiridis, MD, MSc, PhD, FRCS[2,4,5]

1. Department of Mechanical Engineering,
University College London,
Torrington Place, London WC1E 7JE, UK

2. Academic Orthopaedics and Trauma Unit,
Aristotle University Medical School,
University Campus 54 124, Thessaloniki, Greece

3. Medical and Biological Engineering,
School of Engineering,
University of Hull,
Hull, HU6 7RX, UK

4. Academic Department of Orthopaedic and Trauma,
University of Leeds,
Leeds, LS2 9JT, UK

5. Department of Surgery and Cancer, Division of Surgery,
Imperial College London,
London, W12 0HS, UK

Corresponding author:
Mehran Moazen, BSc, PhD, CEng, MIMechE, FHEA
Department of Mechanical Engineering,
University College London,
Torrington Place, London WC1E 7JE, UK
Tel: +44 (0) 208 954 0636
Fax: +44 (0) 208 954 6371
Email: Mehran_Moazen@yahoo.com; M.Moazen@ucl.ac.uk

Application of far cortical locking technology in periprosthetic femoral fracture fixation - a biomechanical study

Abstract

Background: Lack of fracture movement could be a potential cause of periprosthetic femoral fracture (PFF) fixation failures. This study aimed to test whether the use of distal far cortical locking screws reduce the overall stiffness of PFF fixations and allows an increase in fracture movement compared to standard locking screws while retaining the overall strength of the PFF fixations.

Methods: Twelve laboratory models of Vancouver type B1 PFFs were developed. In all specimens the proximal screw fixations were similar, while in six specimens distal locking screws were used, and in the other six specimens far cortical locking screws. The overall stiffness, fracture movement and pattern of strain distribution on the plate were measured in stable and unstable fractures under anatomical one-legged stance. Specimens with unstable fracture were loaded to failure.

Results: No statistical difference was found between the stiffness and fracture movement of the two groups in stable fractures. In the unstable fractures, the overall stiffness and fracture movement of the locking group was significantly higher and lower than the far cortical group, respectively. Maximum principal strain on the plate was consistently lower in the far cortical group and there was no significant difference between the failure loads of the two groups.

Conclusion: The results indicate that far cortical locking screws can reduce the overall effective stiffness of the locking plates and increase the fracture movement while maintaining the overall strength of the PFF fixation construct. However, in unstable fractures, alternative fixation methods e.g. long stem revision might be a better option.

Keywords: fracture stability, fracture movement, strain, stiffness, biomechanics, Vancouver type B1, far cortical locking screw

Running title: Locking versus far cortical locking screw

1. Introduction

Periprosthetic femoral fractures (PFF) occur during or following total hip arthroplasty (THA) [1-5]. It is likely that there will be an increase in the number of these fractures as the number of THAs increases and the lifespan of patients increase [3]. Management of these fractures is challenging due to the presence of the underlying prosthesis. With the introduction of locking plates and their advantage over conventional non-locking plates, i.e. in preserving blood supply [6], their application in the management of PFFs has increased [7, 8]. At the same time, there have been a number of locking plate failures in PFF management [8-11]. Determining the reason behind these failures is challenging. Three main factors are likely to be important: (1) patient-specific factors such as fracture stability and bone quality [12,13]; (2) implant-specific factors such as mechanical properties and design [14,15]; and (3) surgical factors such as bridging length, method of application and fracture reduction [16,17]. Overall, it is widely accepted that both a lack or an excess of fracture movement, dictated by the overall stiffness of the fracture fixation construct, will suppress callus formation, and the fixation will ultimately fail due to high strain under cyclic loading i.e. through mechanical fatigue [18,19].

It has been shown by several groups that locking plates can, depending on how they have been applied, lead to overly rigid fixations that will suppress callus formation

[11,20]. Recently, Bottlang et al. [21] showed that far cortical locking screws, where the screw locks into the plate and bypasses the near cortex, can reduce the effective stiffness of locking plates compared to standard locking screws that are secured in both near and far cortices. They demonstrated this in various laboratory models replicating diaphyseal fracture fixation and in an animal model where distal and proximal locking screws were compared versus far cortical locking screws [21-23]. Their results showed that far cortical locking screws: (1) reduce the overall stiffness of the fracture fixation construct; (2) induce parallel fracture movement; (3) retain the overall stiffness of the constructs; and (4) lead to a more uniform callus formation than normal locking screws. Far cortical locking screws are now commercially available and there is a growing body of literature on their applications [24, 25].

Considering the failure history of locking plates in PFF fixation and the introduction of far cortical locking screws, this study was designed to test the application of the far cortical locking screws in PFF fixations. The main aims of the study were to understand to what extent distal far cortical locking screws: reduce the overall stiffness; increase the fracture movement; alter the pattern of strain distribution on the plate; and affect the overall strength of PFF fixations. Thus this study is essentially asking the same questions as earlier studies that demonstrated the innovation of far cortical locking screw in diaphyseal fracture fixation [21-23], but in the context of PFF fixation. This is necessary because: (1) due to the presence of the prosthesis, the load transfer path with PFF is different to that of an intact femur; (2) in this study only distal far cortical screws are applied compared to proximal and distal far cortical screws.

2. Materials and methods

Specimens: Twelve large, left, fourth-generation composite femurs (Sawbones Worldwide, WA, USA) were used in this study with simulated Vancouver type B1 PFFs, i.e. with the fracture located around the stem with a stable implant and good bone quality [1] fixation. The specimens were prepared by removing the femoral condyles i.e. distal 60 mm of the femur. Then, total hip replacement was performed using a Zimmer CPT femoral stem (Size 2) and Zimtron modular femoral head (28 mm diameter), both manufactured from stainless steel (Zimmer, IN, USA). The stem was inserted into the femoral canal and cemented using Hi-Fatigue G Bone Cement (Zimmer, Sulzer, Switzerland).

To minimize inter-specimen differences due to plate positioning and fracture reduction, each specimen was plated first and then a simulated fracture was created 20 mm below the tip of stem using a band saw. A twelve hole titanium NCB Periprosthetic Proximal Femur Plate (Zimmer, Warsaw, IN, USA) was used (length: 284 mm; thickness: 5 mm; width: 22 mm at the fracture site). The plate has a wide section proximally and a narrow section distally. The wide section allows screw insertion anterior and posterior to the underlying stem while the narrow section allows single screw insertion (see Fig 1A). Six NCB (Non-Contact Bridging) screws were used to fix the plate proximally (outer diameter: 4 mm; length: varying depending on the location from 36-40 mm) while four screws were used distally (outer diameter: 5 mm; length: 40 mm). Three screw holes were left across the fracture gap equivalent to a 100 mm bridging gap [17]. In all twelve specimens the proximal screw fixations were similar, while in six specimens distal Locking screws (Zimmer, Warsaw, IN, USA) were used, and in the other six specimens far cortical locking screws

(MotionLoc, Zimmer, Warsaw, IN, USA) were used (Fig 1B). All screws (proximal and distal) were locked to the plate; the difference between the locking and far cortical locking constructs was the bicortical fixation in the former, but only far cortical fixation in the latter. During plating, spacers were used between the plate and bone to provide a 1 mm plate-bone gap [26].

Loading: The distal 40 mm of the resected distal femur was fixed securely using screws in a cylindrical housing and mounted on a material testing machine (Lloyd Instruments, West Sussex, UK) at 10° adduction in the frontal plane and aligned vertically in the sagittal plane [25,26]. This position simulates anatomical one-legged stance [29]. Constructs were tested initially under axial loads of up to 700 N, corresponding to recommended partial weight bearing i.e. toe touch weight bearing [30]. Loading was applied to the femoral head stem via a hemispherical cup.

Measurements: The stiffness of the specimens was calculated from the slope of the load-displacement data obtained from the material testing machine. Where there was a bilinear stiffening effect, the initial, secondary and overall stiffness were reported. The fracture movement was quantified using two micro-miniature differential variable reluctance transducers (DVRT- LORD MicroStrain, VT, USA). The DVRTs were fixed to the proximal and distal fragments of the fracture where the changes in the voltage (due to displacement) were recorded in LabVIEW (National Instruments, TX, USA) and converted to displacement based on separately calculated calibration data. The accuracy of the DVRTs were 0.001 mm and were placed on the medial and lateral sides of the femur across the fracture. The lateral DVRT was approximately 5 mm from to the plate. The strain on the plate was recorded across the fracture site using a Q100 Electronic Speckle Pattern Interferometry system (ESPI - Dantec Dynamics GmbH, Ulm, Germany). The plate surface was first sprayed with a white spray to create a non-reflective surface (DIFFU-THERM developer, Technische Chemie KG, Herten, Germany). A three leg adaptor was fixed to the plate using X60 two component adhesive (HBM Inc., Darmstadt, Germany) and was used to fix the Q100 sensor to the plate (Fig 1D). During the loading the speckle patterns were recorded via the sensor and were used to calculate the displacement and strain at each loading step using the Istra Q100 2.7 software (Dantec Dynamics GmbH, Ulm, Germany). It must be noted that a preliminary test was conducted on an Aluminium plate under tension where ESPI strain measurements across the plate were validated against theoretical vales. During the load-to-failure test, the first abrupt drop in the load (obtained from the load-displacement data) was recorded as the initial crack (typically seen to be a 17% drop in the load). Ultimate failure was recorded at the point just before catastrophic failure of the construct, which coincided with complete loss of loading (typically leading to a 50% drop in the load).

Testing and analysis: Specimens were first tested with a stable fracture where the fracture gap produced by a band saw was filled with a similar sized slice of synthetic bone. Overall stiffness and fracture movement were recorded for all specimens under axial loading of 500 and 700 N. The lower value was selected to be consistent with previous tests reported in the literature [28,31], however during preliminary tests it was noted a change in slope of the load-deflection graph sometimes occurred at typically 500 N therefore the test was extended to 700 N to capture that effect. The sample with the closest stiffness to the average stiffness of all samples in each group (i.e. locking and far cortical locking) was chosen for strain measurement on the plate across the fracture site. Strain measurement was repeated five times and average of the maximum (first) principal strain across the empty screw hole (averaged over the whole surface as captured by the ESPI system in Fig 1D) was reported. Then, the fracture gap in all samples was increased to 10 mm (i.e. unstable fracture - Fig 1C) and same procedure was repeated. This enlarged gap was used to ensure that no contact occurred at the fracture site under the initial loading up to 700 N, and was similar to previous studies replicating commuted fractures [28, 31]. To ensure a like-for-like comparison of the strain measurements, the same specimens used for the strain measurement with stable fractures were re-used with unstable fracture (Fig 1D). Finally, all specimens with unstable fractures were loaded to failure. Two-tailed, unpaired Student t-test at a level of significance of $p < 0.05$ was used to detect significant differences in the stiffness, fracture movement and load-to-failure data. A statistical analysis was not performed on the strain data since the strain measurements were performed only on one specimen in each group.

3. Results

Stiffness: Under stable fracture conditions, the initial fracture gap (despite being filled with a thin slice of synthetic bone) was seen to be fully closed at approximately 200 N in both the locking and far cortical locking groups (Fig 2A). As a result a bilinear stiffness was observed for both locking (initial stiffness: 346±149 N/mm; secondary stiffness: 1194±215 N/mm; overall stiffness of 660±174 N/mm) and far cortical locking group (initial stiffness: 314±78 N/mm; secondary stiffness: 1273±183 N/mm; overall stiffness: 640±89 N/mm). No difference was detected between the two groups in terms of any measures of fracture stiffness (Fig 3A).

Under unstable fractures (Fig 2B), a bilinear stiffness was again found in the locking group at 200 N (initial stiffness: 345±49 N/mm; secondary stiffness: 550±48 N/mm; overall stiffness: 443±64 N/mm) and in the far cortical locking group at 500 N (initial stiffness: 300±38 N/mm; secondary stiffness: 458±55 N/mm; overall stiffness: 331±27 N/mm). The bi-linearity in the locking group appeared to occur as a result of plate-bone contact at approximately 200 N, while in the far cortical locking group it was a combined effect of far cortical locking screw bending and contacting the near cortex and plate-bone contact. There were statistically significant differences between the secondary (p=0.011) and overall (p=0.003) stiffnesses of the locking and far cortical locking groups (Fig 3B).

Fracture movement: For the stable fracture condition, the lateral fracture movement in both the locking and far cortical locking groups was less than 0.1 mm at 500 and 700 N. The medial fracture movement in the locking and far cortical locking groups was 0.44±0.2 mm and 0.63±0.08 mm at 700 N, which were 23% and 11% higher respectively than the 500 N values. There was no statistical difference between the fracture movement between the two groups, however, the far cortical locking group showed consistently higher fracture movement at both lateral and medial sides (Fig 4A).

In the unstable condition, the lateral fracture movement in both the locking and far cortical locking groups ranged between 0.2-0.6 mm at 500 and 700 N. The medial fracture movement in the locking and far cortical locking groups was 1.1±0.2 mm and 1.6±0.1 mm at 700N, 35% and 28% higher than 500 N values. There was a statistically significant difference in fracture movement between the locking and far cortical locking groups at both 500 N (p=0.000 at the lateral side; p=0.003 at the medial side) and 700 N (p=0.000 at the lateral side; p=0.001 at the medial side), where the far cortical locking group consistently showed higher fracture movement at both lateral and medial sides (Fig 4B).

The ratio of lateral to medial fracture movement was calculated as an indicator of parallel (i.e. axial) fracture movement across the fracture site. This ratio at 700 N for the locking and far cortical locking group in the stable condition was 0.09 and 0.1 (p=0.668) while in the unstable condition was 0.24 and 0.37 (p=0.005) respectively (based on Fig 4B).

Strain: In both the stable and unstable fractures, the overall pattern of maximum principal strain on the plate across the empty screw hole was slightly lower in the far cortical locking group compared to the locking group (Fig 5 and 6). A quantitative analysis of the strain data showed that for a stable fracture, the maximum principal strain in the locking group averaged over the surface that was captured by the ESPI system (as shown in Fig 5 and 6) increased to 284±27 μS (microstrain) as the loading increased to 700 N, while in the far cortical locking arrangement, the maximum principal strain increased to 198±41 μS reaching a limit at 400 N (Fig 7A). In the unstable fracture test, the maximum principal strain at 700 N was 809±89 μS and 638±40 μS for the locking group and far cortical locking group respectively (Fig 7B).

Failure: During the failure tests, for all the locking screw specimens, crack initiation and initial failure occurred at the closest screw to the fracture site on the proximal femoral fragment (at 4656±1067 N). The specimens eventually failed at the bone-cement-stem interface at the proximal femur where the femoral stem dislocated (at 7217±349 N - see Figs 8 and 9). Four of the far cortical locking specimens showed initial cracks at an identical position to the locking specimens (at 6057±923 N) and eventually failed in a similar way to the locking specimens (at 7367±1123 N - see Fig 9). One of the far cortical locking specimens failed at the base of the femur where the construct was held in the cylindrical housing at 2778 N, and another far cortical locking specimen failed at the most distal screw on the distal femoral fragment at 3630 N. Because they failed in a different way, these two samples were not included in the data presented in Fig 9. No statistical difference was found in the failure results between the locking and far cortical locking groups, regardless of whether the two samples were included.

4. Discussion

Far cortical screws applied at both proximal and distal diaphyseal fragments have been shown to increase fracture movement while retaining the overall strength of fracture fixation constructs under pure axial, torsional and bending loads applied to normal fracture specimens [21]. The current study tested whether the same was true with periprosthetic femoral fractures where only distal far cortical locking screws were applied, and the construct was loaded under an anatomically representative one-legged stance. The results show similar findings to the previous study, i.e. distal far cortical locking screws can reduce the overall stiffness of the locking construct and increase the fracture movement while retaining the overall fixation construct strength. However, the increase in the fracture movement and parallel fracture motion in the far cortical locking group compared to the locking group recorded in this study was not as high as that reported where both proximal and distal far cortical locking screws were applied [21].

The far cortical locking screws only reduced the overall stiffness of fixation of the unstable fractures. With a stable fracture, following the initial contact at the fracture gap, no difference was observed between the far cortical locking and locking groups. It is also noteworthy that the initial stiffness of the far cortical locking group was still slightly lower than the locking group. However, in the unstable fracture, the far cortical locking screws at the near cortex flexed elastically due to the enlarged gap, delaying the plate-bone contact that occurred at the locking group at about 200 N, and hence reduced the overall construct stiffness [see also 31]. Achieving a perfect fracture reduction is clinically challenging and it is likely that in the majority of cases there will be a small fracture gap remaining post-operatively. In these cases, the constructs will behave in a more similar way to the unstable fracture group in this study and, depending on the size of the gap, fracture stability will vary.

Medial fracture movement in the stable fracture group was in the range of ca. 0.2-0.6 mm while on the lateral side it was less than 0.1 mm. These movements are due to inadequate fracture reduction, occurring here because of incomplete filling of the initial fracture gap as described previously. The similarity between the initial stiffness of the stable versus unstable fracture groups (for both the locking and far cortical locking groups) confirms this. At the same time, while there was no statistical significant difference between the fracture movement of the locking and far cortical locking groups in the stable fractures, there was a significant difference between the two groups in the unstable fractures. Considering the ratio of the lateral to medial fracture movement as an indicator of parallel fracture movement, the far cortical locking group showed higher parallel fracture movement i.e. 0.24 versus 0.37 at 700 N in the unstable fracture for locking and far cortical locking respectively (based on Fig 4B). This was similar to the finding of Doornink et al. [23] who compared the far cortical locking and locking screws in distal femoral fracture fixations. Their results showed that at 800 N axial loading the lateral to medial fracture movement ratio was 0.53 and 0.90 for locking and far cortical locking respectively. The lower parallel fracture movement in the far cortical locking group in this study compared to the value reported by Doornink et al. [23] could be due to various differences between the two studies. Nevertheless, higher parallel fracture movement in the far cortical locking compare to locking screws has been shown to induce larger and more uniform callus formation [22].

From a clinical point of view, considering that a titanium plate and screws were used in this study and tested under post-operative load-bearing corresponding to toe touch weight bearing, data obtained in this study suggests that: (1) with stable fractures, application of far cortical locking screws can increase fracture movement; (2) with unstable fractures or where large bridging lengths need to be considered, both locking and far cortical locking screws can increase fracture movement beyond the suggested threshold for healing i.e. 0.2-1 mm [18,19,32,33] and this effect could be amplified at higher post-operative load bearings. Indeed, previous studies suggest that in such cases, revision to a long stem or additional grafting might be a better option [10, 34-36].

When the first principal strain on the plate across the empty screw holes are considered, as expected, the strain in the stable fracture group was lower than the unstable group. It was interesting that lower level of strain was recorded in the far cortical locking group compare to the locking group (Fig 5 and 6). However, previous finite element analysis studies [37,38] have shown that far cortical locking screws are under higher strain compared to locking screws. Given the fracture movement data obtained in this study and, in line with previous studies of Bottlang et al. [21, 22] for stable fractures, it is possible that the fracture would heal before mechanical failure of the screws. With the unstable fractures, the plate itself is under higher strain across the empty screw holes. Nevertheless, the study of Bottlang et al. [25] did not show either screw or plate failure in thirty-one distal fractures fixed with NCB Polyaxial Locking Plate System and far cortical locking screws.

A consistent pattern of crack initiation at the closest screw to the fracture site on the proximal femoral fragment was observed in the locking group and four of the far cortical locking specimens. While previous finite element studies have shown high stress concentration in this region on the bone, to the best of our knowledge most of the clinical studies report failures of PFF fixations across the empty screw hole on the plate [9-11]. This discrepancy is not unique to the present study, and is in fact common between biomechanical studies [14,27].

There were several limitations in the present study that might have contributed to this discrepancy. The properties of the composite femurs used in this study, could have been higher than those observed clinically, especially in the case of osteoporotic patients. Furthermore while the stiffness of these composite femurs may well be optimised for general testing of implant performance, the many other characteristics of bone, such as failure strength and screw pull-out strengths may not be. It is also well established that *in vivo* bone responds to the mechanical strain, and such a response together with the effect of muscle forces, knee joint movement and cyclic loading that occurs *in vivo* were not included in this study. Acting in combination, these factors could potentially lead to increased micromotion at the screw-bone interface and higher implant strains in vivo, and care should therefore be taken in their extrapolation to the clinical setting. However, the advantage of using these composite femurs is that they are consistent with minimum variability between individual bones, unlike natural femurs. Furthermore, any simplifications and limitations in the study were the same for both the locking and far cortical locking screws, therefore the relative comparisons made between the two screw designs in the case of PFF fixations are likely to remain valid.

In conclusion, this study suggests that distal far cortical locking screws can reduce the overall stiffness of the locking constructs in PPF fixation and increase the fracture movement while retaining the overall construct strength. Further, it was found that in unstable fractures, and where large bridging length are required, both locking and far cortical locking screws applied with titanium plates might induce fracture movements beyond the threshold required to promote callus formation, in which case long stem revision might be a better option.

References

1. Duncan CP, Masri BA. Fractures of the femur after hip replacement. Instr Course Lect 1995; 44:293-304.
2. Parvizi J, Rapuri VR, Purtill JJ, et al. Treatment protocol for proximal femoral periprosthetic fractures. J Bone Joint Surg [Am] 2004;86:8-16.
3. Lindahl H, Malchau H, Oden A, et al. Risk factors for failure after treatment of a periprosthetic fracture of the femur. J Bone Joint Surg [Br] 2006; 88:26-30.
4. Mont MA, Maar DC, Fractures of the ipsilateral femur after hip arthroplasty. A statistical analysis of outcome based on 487 patients. J Arthroplasty 1994; 9:511-9.
5. Inngul C, Enocson A, Postoperative periprosthetic fractures in patients with an Exeter stem due to a femoral neck fracture: cumulative incidence and surgical outcome. Int Orthop 2014; in press.
6. Perren SM. Evolution of the internal fixation of long bone fractures. The scientific basis of biological internal fixation: choosing a new balance between stability and biology. J Bone Joint Surg Br 2002;84:1093-110.
7. Niikura T, Sakurai A, Oe K, et al. Clinical and radiological results of locking plate fixation for periprosthetic femoral fractures around hip arthroplasties: a retrospective multi-center study. J Orth Sci 2014;19:984-90.
8. Graham SM, Moazen M, Leonidou A, et al. Locking plate fixation for Vancouver B1 periprosthetic femoral fractures: A critical analysis of 135 cases. J Orth Sci 2013;18:426-36.
9. Buttaro MA, Farfalli G, Paredes Nunez M, et al. Locking compression plate fixation of Vancouver type-B1 periprosthetic femoral fractures. J Bone Joint Surg [Am] 2007; 89:1964-9.

10. Erhardt JB, Grob K, Roderer G, et al. Treatment of periprosthetic femur fractures with the non-contact bridging plate: a new angular stable implant. Arch Orthop Trauma Surg 2008;128:409-16.

11. Moazen M, Jones AC, Leonidou A, et al. Rigid versus flexible plate fixation for periprosthetic femoral fracture - computer modelling of a clinical case. Med Eng Phys 2012; 34:1041-8.

12. Claes L, Eckert-Hubner K, Augat P. The fracture gap size influences the local vascularization and tissue differentiation in callus healing. Langenbecks Arch Surg 2003; 388:316-22.

13. Leonidou A, Moazen M, Lepetsos P, et al. The biomechanical effect of bone quality and fracture topography on locking plate fixation in periprosthetic femoral fractures. Injury 2015; 46:213-17.

14. Lenz M, Gueorguiev B, Joseph S, et al. Angulated locking plate in periprosthetic proximal femur fractures: biomechanical testing of a new prototype plate. Arch Orthop Trauma Surg 2012;132:1437-44

15. Wahnert D, Schroder R, Schulze M, et al. Biomechanical comparison of two angular stable plate constructions for periprosthetic femur fracture fixation. Int Orthop 2014;38:47-53.

16. Dennis MG, Simon JA, Kummer FJ, et al. Fixation of periprosthetic femoral shaft fractures occurring at the tip of the stem: a biomechanical study of 5 techniques. J Arthroplasty 2000;15:523-8.

17. Stoffel K, Dieter U, Stachowiak G, et al. 2003. Biomechanical testing of the LCP--how can stability in locked internal fixators be controlled? Injury 2003;34 Suppl 2:B11-9.

18. Goodship AE, Kenwright J. The influence of induced micromovement upon the healing of experimental tibial fractures. J Bone Joint Surg [Br] 1985; 67:250-5.

19. Augat P, Merk J, Ignatius A, et al. Early, full weight bearing with flexible fixation delays fracture healing. Clin Orthp Relat Res 1996; 328:194-202.

20. Lujan TL, Henderson CE, Madey SM, et al. Locked plating of distal femur fracture leads to inconsistent and asymmetric callus formation. J Orthop Trauma 2010; 24:156-62.

21. Bottlang M, Doornink J, Fitzpatrick DC, et al. Far cortical locking can reduce stiffness of locked plating constructs while retaining construct strength. J Bone Joint Surg Am 2009;91:1985-94.

22. Bottlang M, Doornink J, Lujan TJ, et al. Effects of construct stiffness on healing of fractures stabilized with locking plates. J Bone Joint Surg [Am]. 2010;92:12-22.

23. Doornink J, Fitzpatrick DC, Madey SM, et al. Far cortical locking enables flexible fixation with periarticular locking plates. J Orthop Trauma 2011; 25:S29-S34.

24. Ries Z, Hansen K, Bottlang M, et al. Healing results of periprosthetic distal femur fractures treated with far cortical locking technology: a preliminary retrospective study. Iowa Orthop J 2013;33:7-11.

25. Bottlang M, Fitzpatrick DC, Sheerin D, et al. Dynamic fixation of distal femur fractures using far cortical locking screws: a prospective observational study. J Orthop Trauma 2014;28:181-8.

26. Ahmad M, Nanda R, Bajwa AS, et al. Biomechanical testing of the locking compression plate: When does the distance between bone and implant significantly reduce construct stability? Injury 2007; 38:358-64.

27. Zdero R, Walker R, Waddell JP, et al. Biomechanical evaluation of periprosthetic femoral fracture fixation. J Bone Joint Surg [Am] 2008; 90:1068-77.

28. Moazen M, Jones AC, Jin Z, et al. Periprosthetic fracture fixation of the femur following total hip arthroplasty: a review of biomechanical testing. Clin Biomech 2011; 26:13-22.

29. Bergmann G, Deuretzbacher G, Heller M, et al. Hip contact forces and gait patterns from routine activities. J Biomech 2001; 34:859-71.

30. Ryf CR, Arraf J: Postoperative fracture treatment: general considerations. p. 447. In Ruedi TP, Buckley RE, Moran CG, eds. AO principal of fracture management, 2ed. Davos: AO Publishing; 2007.

31. Moazen M, Mak JH, Etchels LW, et al. The effect of fracture stability on the performance of locking plate fixation in periprosthetic femoral fractures. J Arthroplasty 2013;28:1589-95.

32. Egol KA, Kubiak EN, Fulkerson E, et al. Biomechanics of locked plates and screws. J Orthop Trauma 2004; 18:488-93.

33. Claes L, Wilke H-J, Augat P, et al. Effect of dynamization of gap healing of diaphyseal fractures under external fixation. Clin Biomech 1995; 8:227-34.

34. Haddad FS, Duncan CP, Berry DJ, et al. Periprosthetic femoral fractures around well-fixed implants: use of cortical onlay allografts with or without a plate. J Bone Joint Surg [Am] 2002; 84:945-50.

35. Moazen M, Mak JH, Etchels LW, et al. Periprosthetic femoral fracture - a biomechanical comparison between Vancouver type B1 and B2 fixation methods. J Arthroplasty 2014;29(3):495-500.

36. Sariyilmaz K, Dikici F, Dikmen G, et al. The Effect of Strut Allograft and Its Position on Vancouver Type B1 Periprosthetic Femoral Fractures: A Biomechanical Study. J. Arthroplasty 2014;29:1485-90.

37. Bottlang M, Feist F. Biomechanics of far cortical locking. J Orthop Trauma 2011;25 Suppl 1:S21-8.

38. Moazen M, Mak JH, Jones AC, et al. Evaluation of a new approach for modelling the screw–bone interface in a locking plate fixation - a corroboration study. Proc Inst Mech Eng H 2013;227:746-56.

Acknowledgments

This work was supported by Zimmer (SA, Switzerland). We would like to thank Patric Sommer, Robin Chapman, Gavin Giles and Jeffery Rodman for their assistance during the experimental work.

Figure legends

Fig. 1 An overview of the study: (A) lateral view of the plate and anterior-posterior radiograph of a locking periprosthetic femoral fracture fixation construct; (B) comparing distal Locking versus Far cortical locking screws; (C) comparing stable versus unstable fractures; (D) a summary of the parameters recorded in this study, also highlighting the electronic speckle pattern interferometry sensor (attached to the plate) and micro-miniature differential variable reluctance transducers (attached to the bone).

Fig. 2 Graph of the load-displacement data recorded under stable (A) and unstable (B) fractures for the locking and far cortical locking group.

Fig. 3 Summary of the initial, secondary and overall stiffness values calculated under stable (A) and unstable (B) fractures for the locking and far cortical locking groups. * highlight statistical significance between the corresponding groups ($p<0.05$).

Fig. 4 Summary of the fracture movement data under stable (A) and unstable (B) fractures for the locking and far cortical locking groups at the lateral (lat) and medial (med) side at 500 and 700 N. * highlight statistical significance between the corresponding groups ($p<0.05$).

Fig. 5 Comparison between the pattern of maximum principal strain across the empty screw hole on the fracture plate, between the locking and far cortical locking group for stable fractures at 500 and 700 N.

Fig. 6 Comparison between the pattern of maximum principal strain across the empty screw hole on the fracture plate, between the locking and far cortical locking group for unstable fractures at 500 and 700 N.

Fig. 7 Summary of the average maximum principal strain across the empty screw hole on the fracture plate for the locking and far cortical locking group under stable (A) and unstable (B) fracture conditions during loading up to 700 N.

Fig. 8 An example of a locking sample load to failure test, highlighting the crack initiation at about 4000 N and ultimate failure at about 6900 N.

Fig. 9 Summary of the load to failure data, highlighting the crack initiation and ultimate failure loads of the unstable fractures for the locking and far cortical locking groups. No statistical difference was observed between the aforementioned groups.

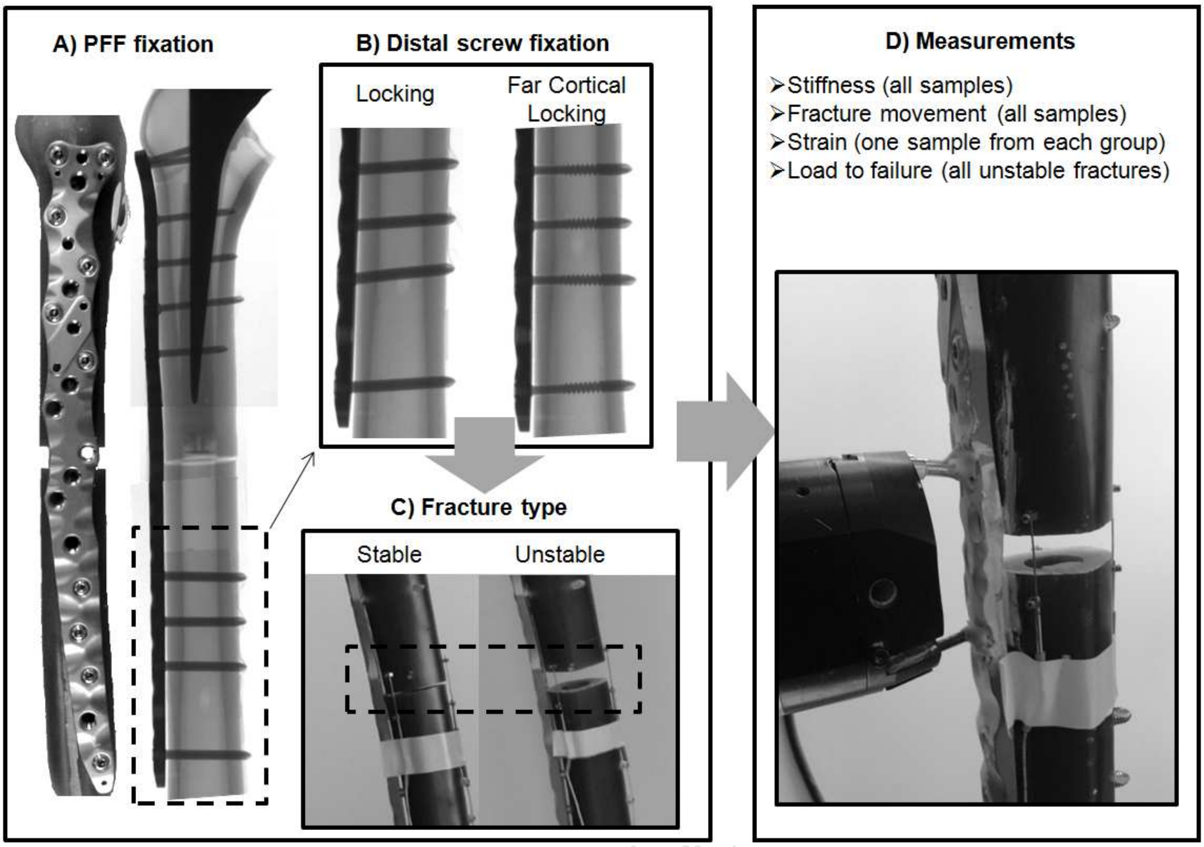

A) PFF fixation
B) Distal screw fixation
Locking
Far Cortical Locking
C) Fracture type
Stable
Unstable
D) Measurements
➢Stiffness (all samples)
➢Fracture movement (all samples)
➢Strain (one sample from each group)
➢Load to failure (all unstable fractures)

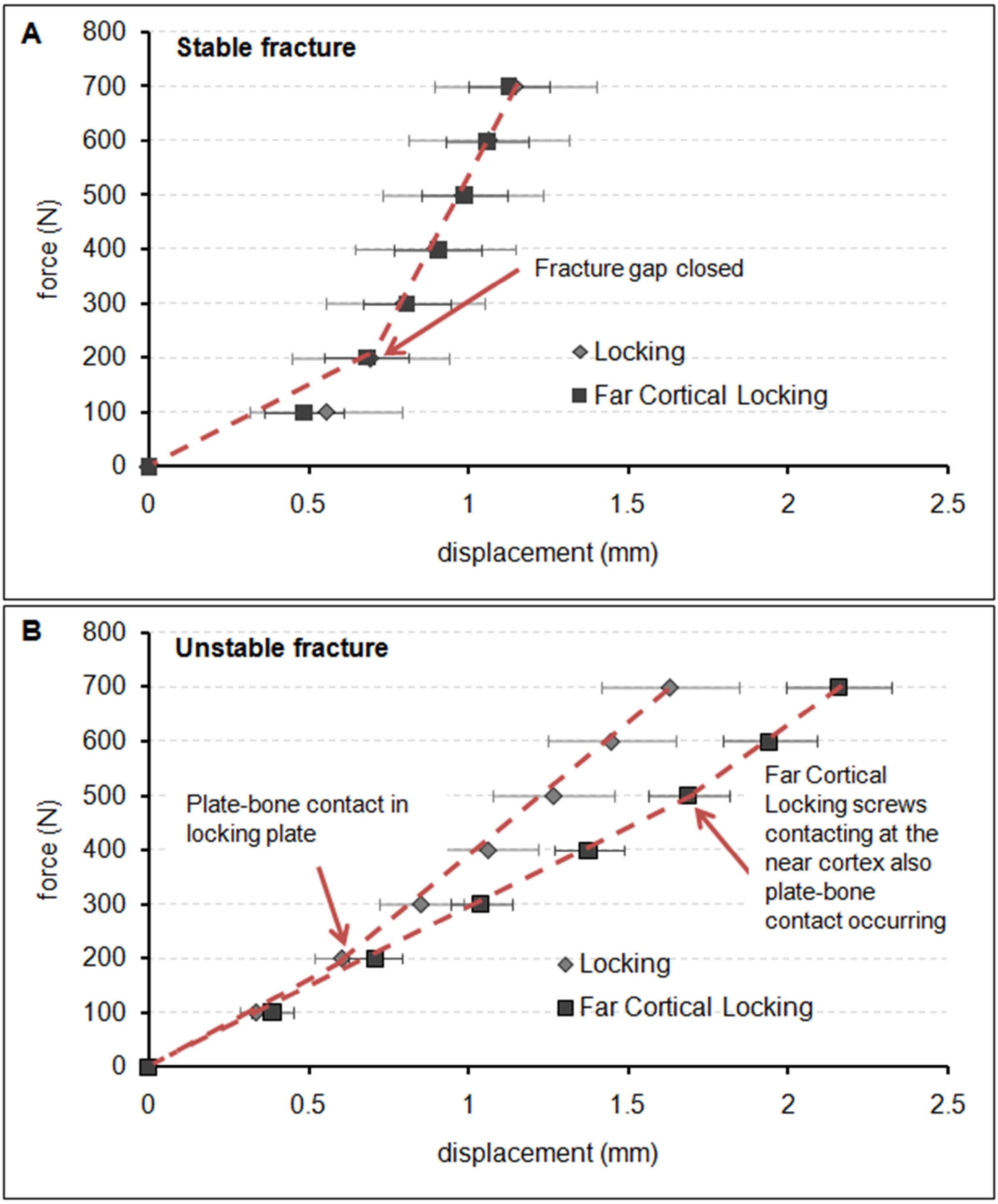
A
Stable fracture
force (N)
displacement (mm)
0
100
200
300
400
500
600
700
800
0
0.5
1
1.5
2
2.5
Fracture gap closed
Locking
Far Cortical Locking
B
Unstable fracture
force (N)
displacement (mm)
0
100
200
300
400
500
600
700
800
0
0.5
1
1.5
2
2.5
Plate-bone contact in locking plate
Far Cortical Locking screws contacting at the near cortex also plate-bone contact occurring
Locking
Far Cortical Locking

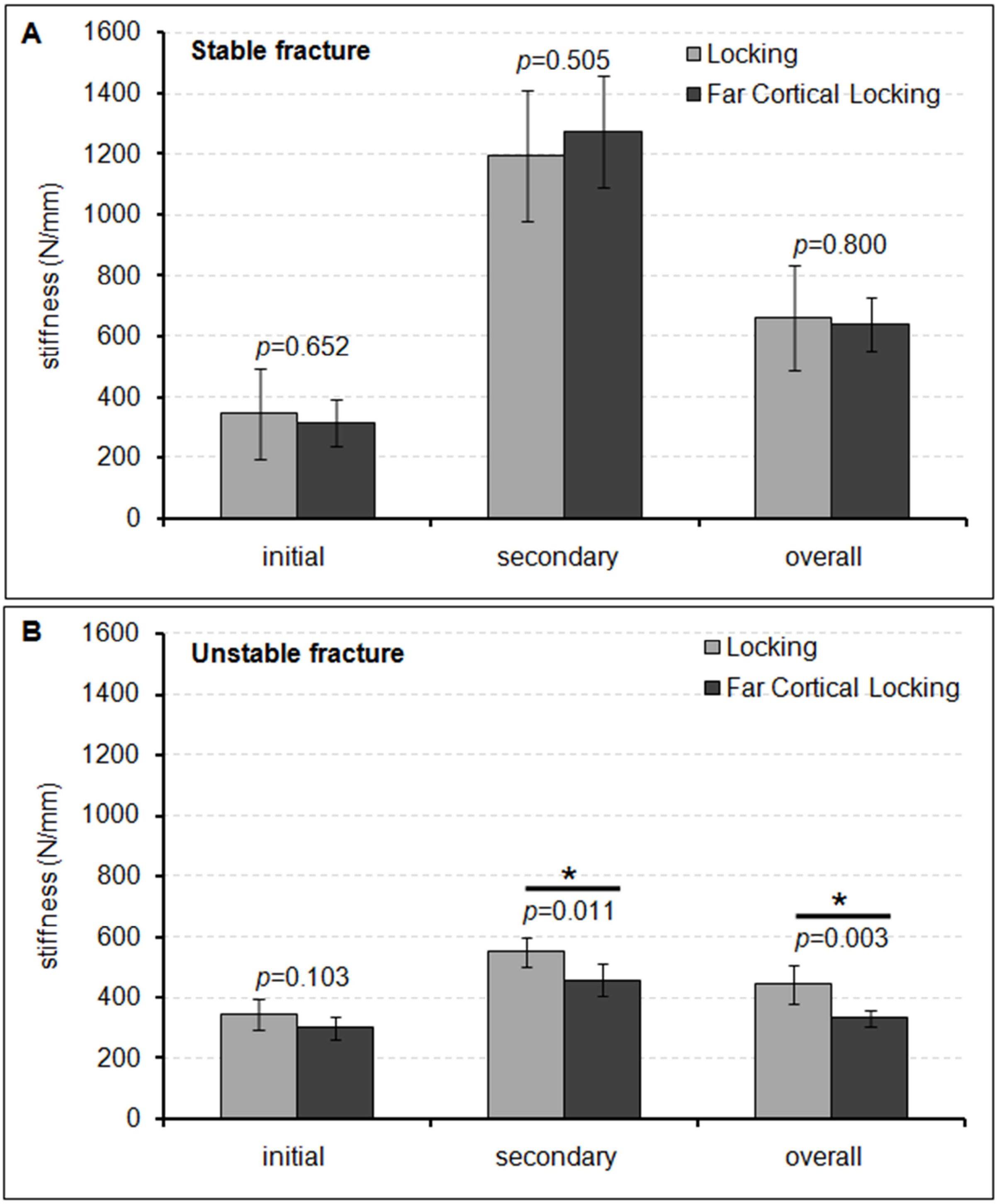
A
Stable fracture
Locking
Far Cortical Locking
stiffness (N/mm)
1600
1400
1200
1000
800
600
400
200
0
p=0.652
p=0.505
p=0.800
initial
secondary
overall
B
Unstable fracture
Locking
Far Cortical Locking
stiffness (N/mm)
1600
1400
1200
1000
800
600
400
200
0
p=0.103
*
p=0.011
*
p=0.003
initial
secondary
overall

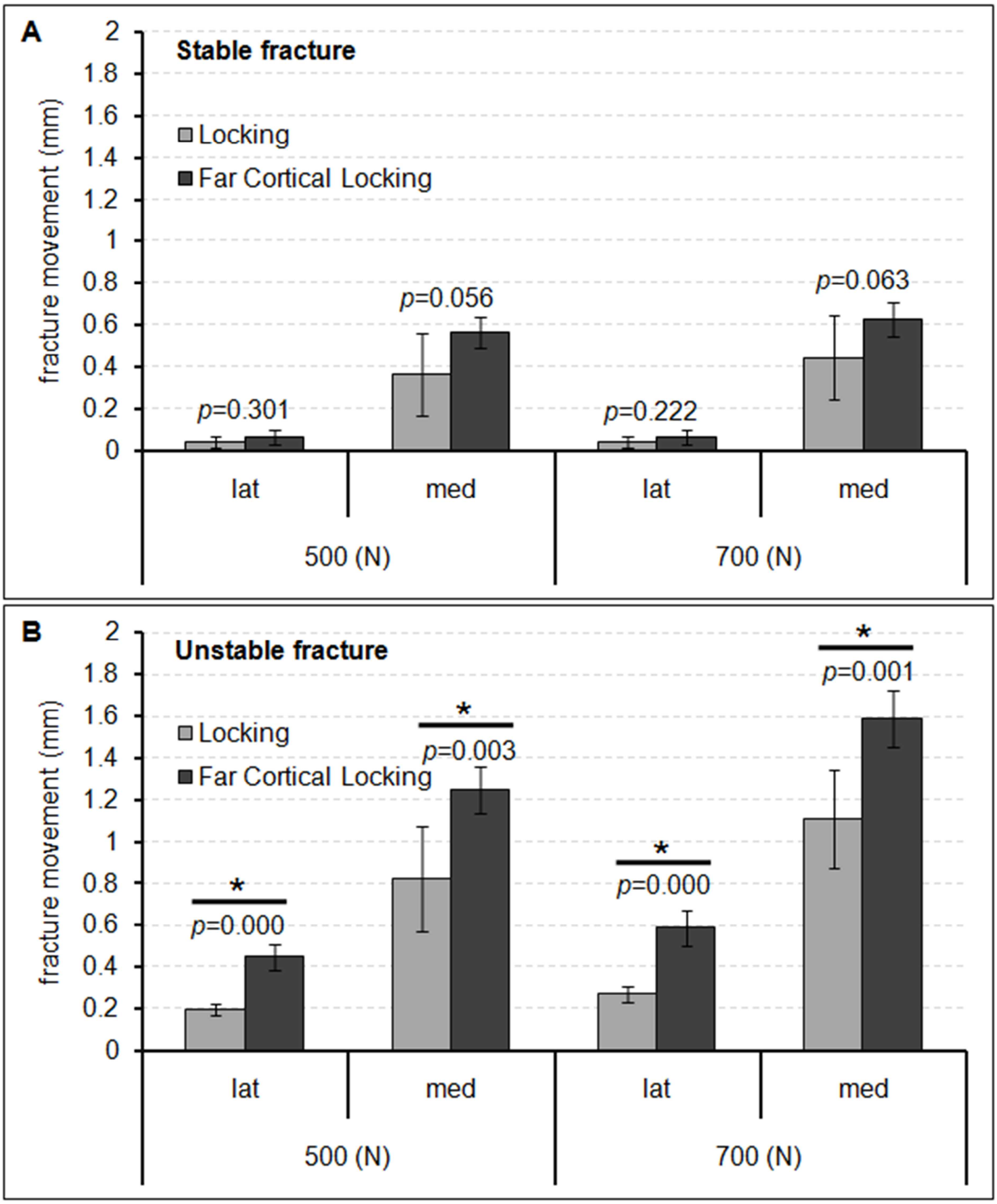
A
Stable fracture
Locking
Far Cortical Locking
fracture movement (mm)
2
1.8
1.6
1.4
1.2
1
0.8
0.6
0.4
0.2
0
p=0.301
p=0.056
p=0.222
p=0.063
lat
med
lat
med
500 (N)
700 (N)
B
Unstable fracture
Locking
Far Cortical Locking
fracture movement (mm)
*
p=0.000
*
p=0.003
*
p=0.000
*
p=0.001
lat
med
lat
med
500 (N)
700 (N)

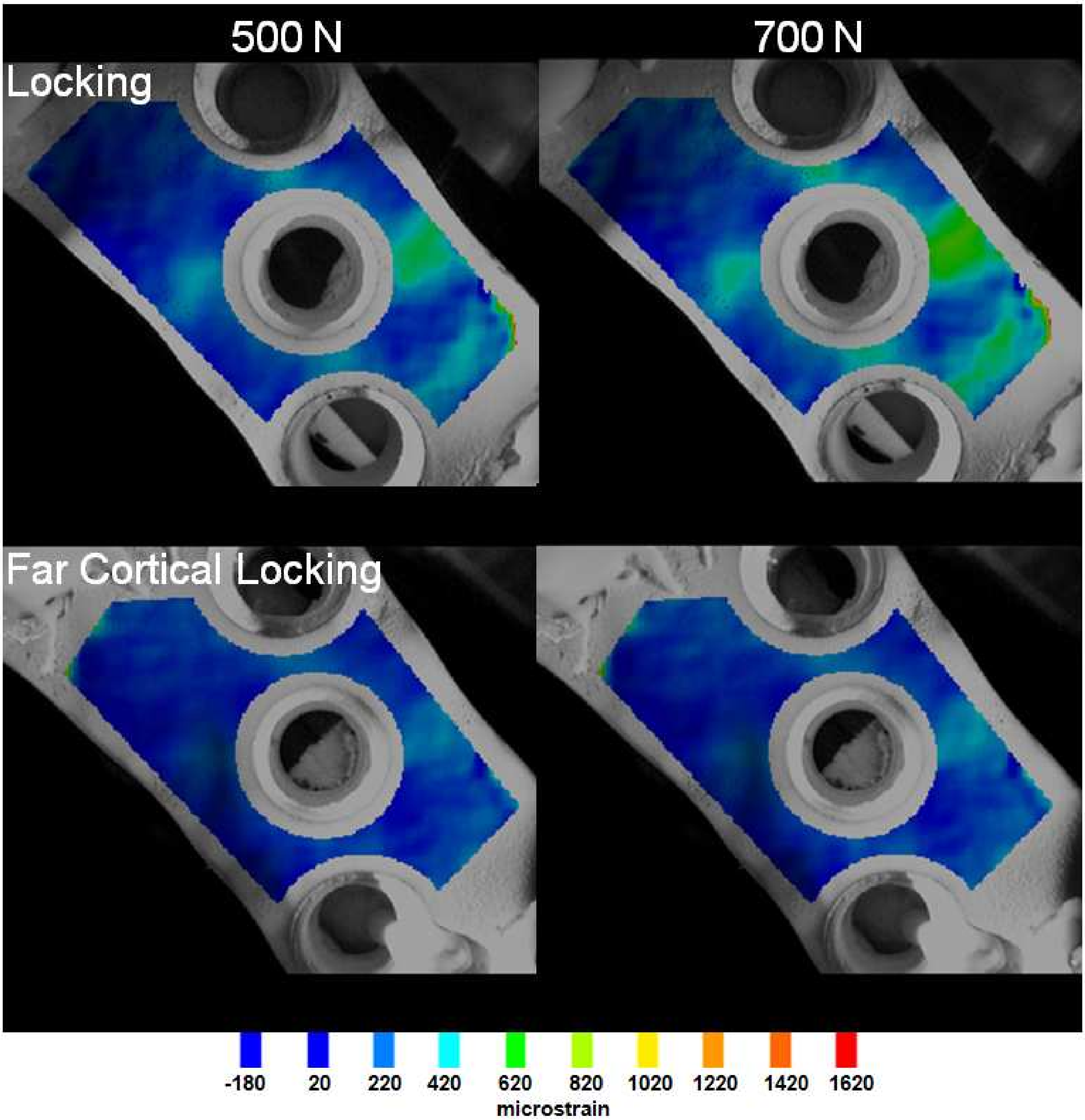
500 N
700 N
Locking
Far Cortical Locking
-180
20
220
420
620
820
1020
1220
1420
1620
microstrain

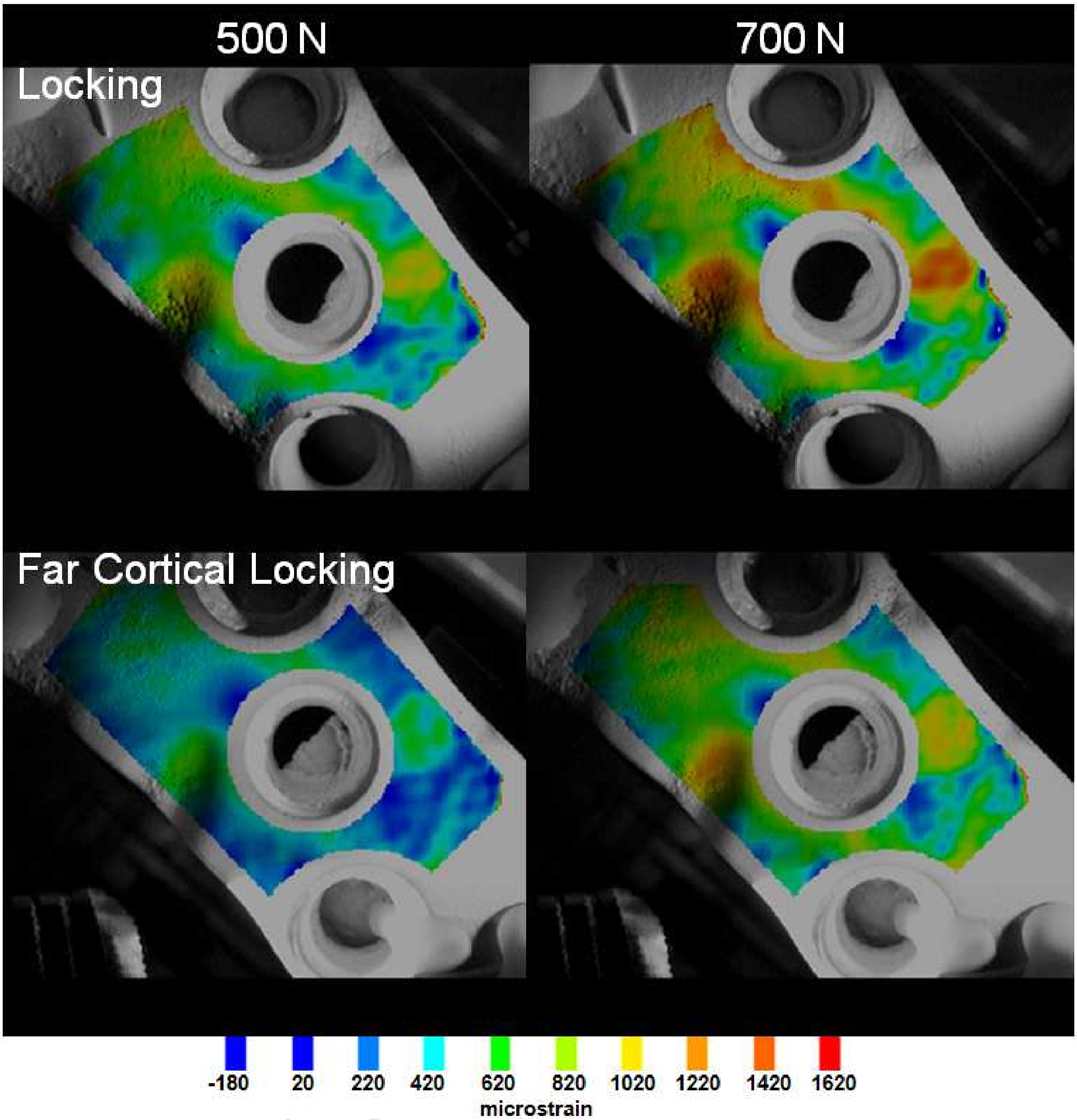
500 N
700 N
Locking
Far Cortical Locking
-180
20
220
420
620
820
1020
1220
1420
1620
microstrain

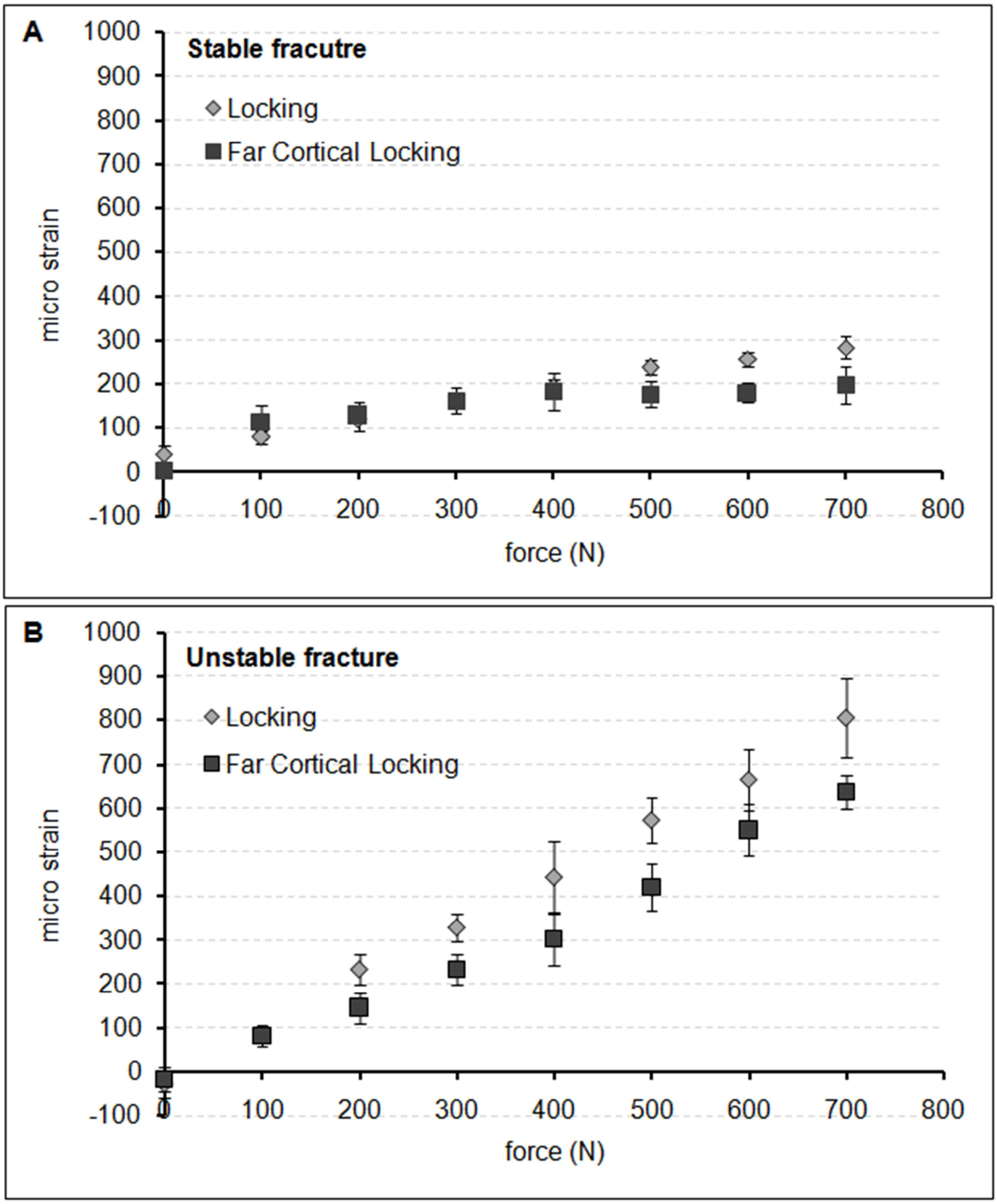
A
Stable fracutre
Locking
Far Cortical Locking
micro strain
force (N)
B
Unstable fracture
Locking
Far Cortical Locking
micro strain
force (N)

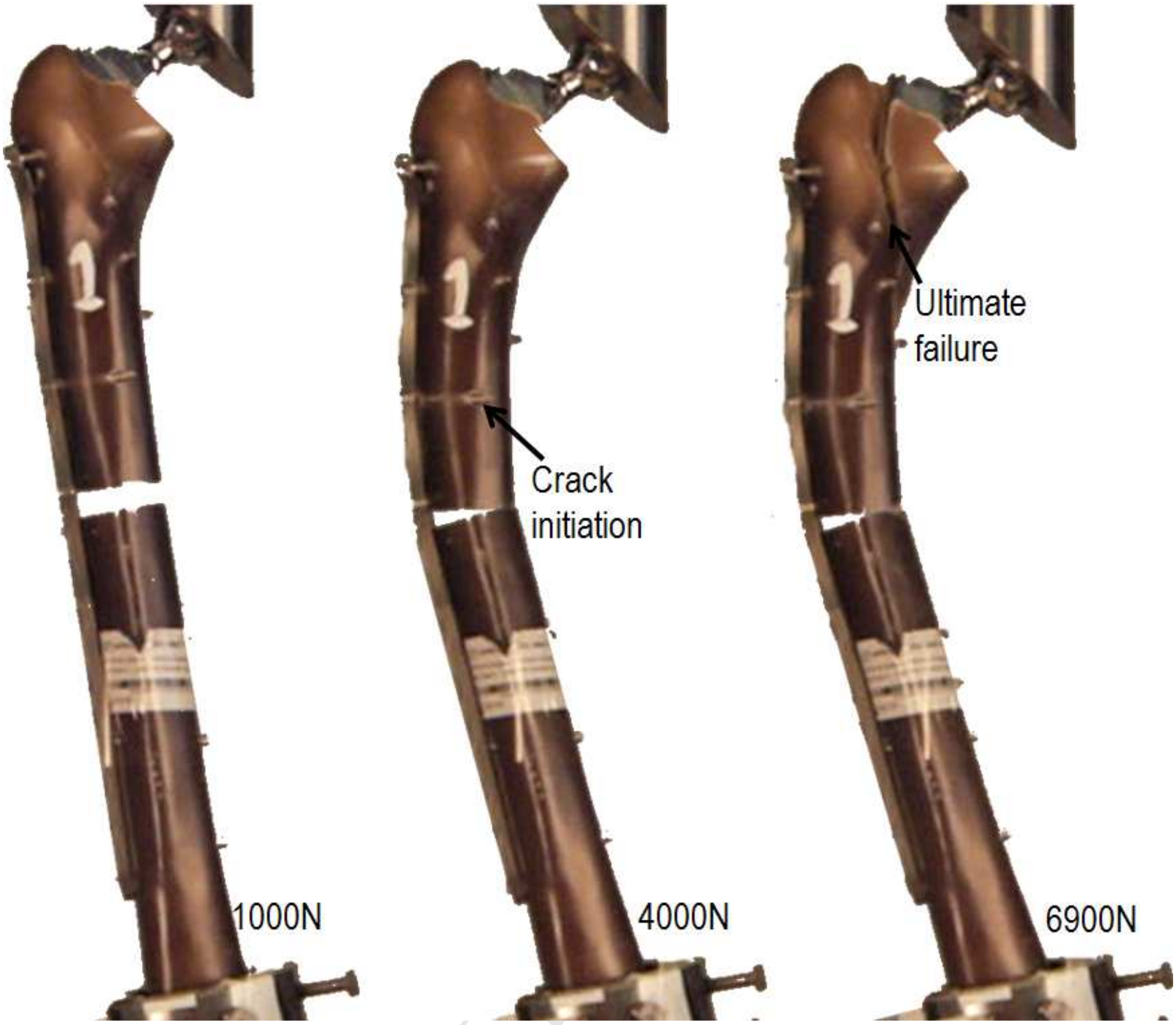
Crack
initiation
Ultimate
failure
1000N
4000N
6900N

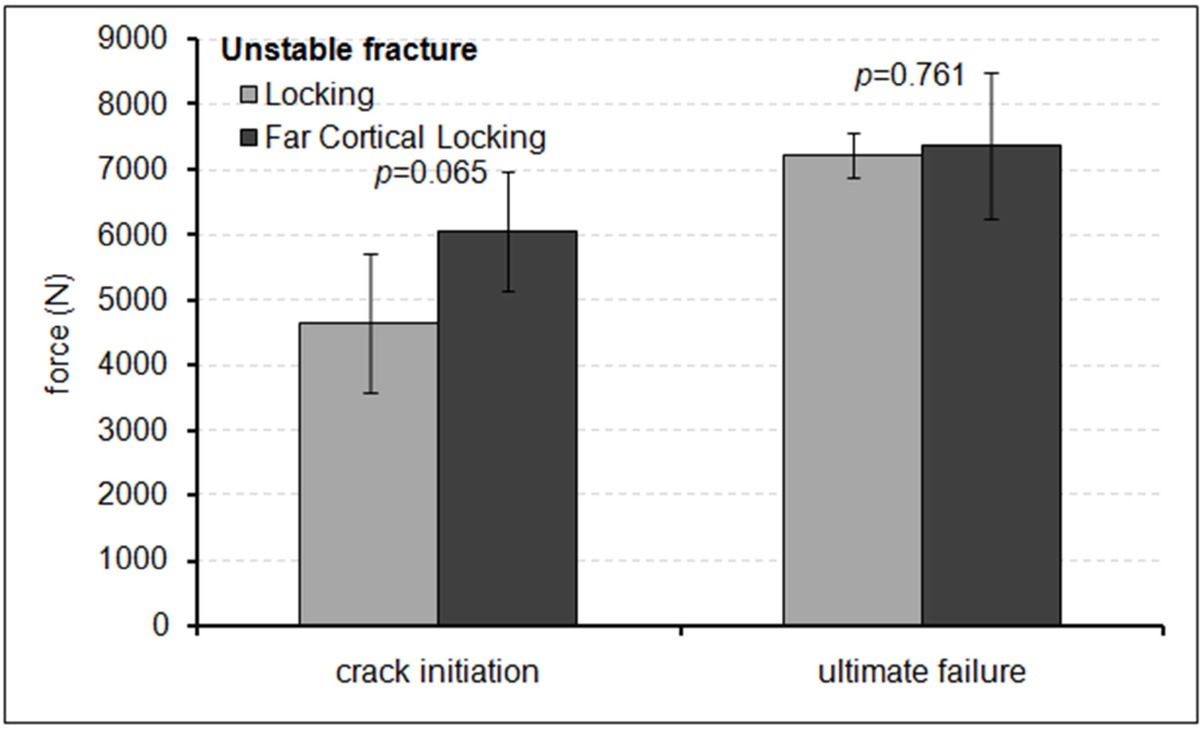

Unstable fracture
Locking
Far Cortical Locking
p=0.065
p=0.761
9000
8000
7000
6000
5000
4000
3000
2000
1000
0
force (N)
crack initiation
ultimate failure